Bioorganic Chemistry 107 (2021) 104636

Contents lists available at ScienceDirect

Bioorganic Chemistry

journal homepage: www.elsevier.com/locate/bioorg

Oxaliplatin derived monofunctional triazole-containing platinum(II) complex counteracts oxaliplatin-induced drug resistance in colorectal cancer

Yaru Li [a,1], Ziru Sun [a,1], Yujun Cui [a,b], Heming Zhang [a,d], Shunjie Zhang [a], Xinyu Wang [a], Shengnan Liu [a,*], Qingzhi Gao [a,c,*]

[a] School of Pharmaceutical Science and Technology and Institute of Molecular Plus, Tianjin Key Laboratory for Modern Drug Delivery & High-Efficiency, Tianjin University, 92 Weijin Road, Nankai District, Tianjin 300072, PR China
[b] Transplantation Center, Tianjin First Central Hospital, 24 Fukang Road, Nankai District, Tianjin 300192, PR China
[c] Department of Biology, Gudui BioPharma Technology Inc, 5 Lanyuan Road, Huayuan Industrial Park, Tianjin 300384, PR China
[d] Central Institute of Pharmaceutical Research, CSPC Pharmaceutical Group, 226 Huanhe Road, Shijiazhuang, Hebei 050035, PR China

ARTICLE INFO

Keywords:
Monofunctional Pt(II) complex
DNA binding
Oxaliplatin
Drug resistance
Glutathione

ABSTRACT

Oxaliplatin-based chemotherapy is the current standard of care in adjuvant therapy for advanced colorectal cancer (CRC). But acquired resistance to oxaliplatin eventually occurs and becoming a major cause of treatment failure. Thus, there is an unmet need for developing new chemical entities (NCE) as new therapeutic candidates to target chemotherapy-resistant CRC. Novel Pt(II) complexes were designed and synthesized as cationic monofunctional oxaliplatin derivatives for DNA platination-mediated tumor targeting. The complex Ph-glu-Oxa sharing the same chelating ligand of diaminocyclohexane (DACH) with oxaliplatin but is equally potent in inhibiting the proliferation of HT29 colon cancer cells and its oxaliplatin-resistant phenotype of HT29/Oxa. The *in vivo* therapeutic potential of Ph-glu-Oxa was confirmed in oxaliplatin-resistant xenograft model demonstrating the reversibility of the drug resistance by the new complex and the efficacy was associated with the unimpaired high intracellular drug accumulation in HT29/Oxa. Guanosine-5′-monophosphate (5′-GMP) reactivity, double-strand plasmid DNA cleavage, DNA-intercalated ethidium bromide (EB) fluorescence quenching and atomic force microscopy (AFM)-mediated DNA denaturing studies revealed that Ph-glu-Oxa was intrinsically active as DNA-targeting agent. The diminished susceptibility of the complex to glutathione (GSH)-mediated detoxification, which confers high intracellular accumulation of the drug molecule may play a key role in maintaining cytotoxicity and counteracting oxaliplatin drug resistance.

1. Introduction

Oxaliplatin has a unique chiral bidentate chelating ligand of (1*R*,2*R*)-cyclohexane-1,2-diamine (DACH) which results in more effective DNA deformation and greater cytotoxicity in metastatic colorectal cancers (CRC) [1]. The DACH ligand also prevents the DNA mismatch repair (MMR) from oxaliplatin-DNA adducts therefore to abolish cross-resistance between oxaliplatin and other platinum compounds [2]. Compared to cisplatin, oxaliplatin produces fewer DNA adducts at same drug concentrations but induces more DNA lesion in several different cell lines [3], which is implying the significant contribution of the chiral DACH ligand in enhancing cytotoxicities [4]. Despite the great improvement in the treatment outcome of CRC, the intrinsic or acquired oxaliplatin resistance is still a major clinical challenge [5–7].

The molecular mechanisms involved in oxaliplatin resistance are recognized to be multifactorial, including intracellular uptake, drug detoxification, DNA repair alteration and many other biological events [7]. Therefore, a combination approach might be a promising strategy to combat or circumvent the drug resistance. For DNA repair alteration, although oxaliplatin exhibits less cross-resistance to cis- and carboplatin as oxaliplatin-DNA adducts can bypass the recognition and repair of MMR, however, *in vitro* study has demonstrated that DNA damages

* Corresponding authors at: School of Pharmaceutical Science and Technology and Institute of Molecular Plus, Tianjin Key Laboratory for Modern Drug Delivery & High-Efficiency, Tianjin University, 92 Weijin Road, Nankai District, Tianjin 300072, PR China (Q. Gao).
E-mail addresses: shengnan_liu@tju.edu.cn (S. Liu), qingzhi@tju.edu.cn (Q. Gao).
[1] These authors equally contributed to this work.

https://doi.org/10.1016/j.bioorg.2021.104636
Received 28 October 2020; Received in revised form 3 January 2021; Accepted 4 January 2021
Available online 8 January 2021

generated by both cisplatin and oxaliplatin can be repaired with similar effectiveness by another system called nucleotide excision repair (NER) [8]. Therefore, there are still some potential new strategies worthwhile to consider on modulating DNA adduct formation while designing new oxaliplatin analogs. Lippard and other groups have reported cisplatin derived monofunctional platinum(II) complexes which bind with DNA at a single site, but exhibit significantly greater activity than cisplatin due to additional N-heterocycle ligand may alter not only the DNA binding conformation of the drug molecule, but also the reactivity toward sulfur-containing detoxicates [9,10]. More recent report demonstrated that cisplatin-based monofunctional platinum(II) complex like phenanthriplatin is causing unique or enhanced effects on modulating some oncogenes involved in the regulation of cytoskeleton, cell migration, and proliferation, that leading to improved clinical outcome and safety profiles compared to its parent drug cisplatin. These study results shed light on the importance of monofunctional platinum(II) complex in the development of new generation of platinum-based anticancer agents.

In this study, to address the oxaliplatin resistance, we aimed to design new analogs of oxaliplatin that could regain potency for CRC treatment. The strategy is to focus on the drug detoxification process which involves the glutathione (GSH)-mediated Pt(II) conjugation and subsequent drug efflux [11,12]. Increased or activated synthesis of GSH as well as cysteine-rich metallothioneins is considered to be involved in cellular platinum drug sequestration, and GSH has been used as clinical modality to minimize the cumulative side toxicities associated with oxaliplatin therapy [13–15]. The rationale for the molecular design in the current study is driven by the following objectives: (1) keep the DACH bidentate chelating ligand to maintain the potential unique cytotoxicity profile of the Pt(II) complex with CRC selectivity, (2) change oxaliplatin into a monofunctional cationic complex to increase the water solubility and physiological stability, (3) diminish the nucleophilic vulnerability toward GSH by installing a sterically hindered chelating ligand, which may also contribute to improved DNA denaturation (Scheme 1).

2. Results and discussion

2.1. Chemistry

The preparation of the DACH containing monofunctional cationic Pt(II) complexes were carried out by using dichloro-[(1*R*,2*R*)-1,2-cyclohexanediamine-N-N']platinum(II) ([Pt(DACH)Cl_2]) reacting with corresponding triazole and glycoconjugated phenyltriazole as additional chelating ligand in N,N-dimethylformamide (DMF) in the presence of silver nitrate as described in the experimental section. Detailed information for the characterization of the complexes was provided in Supplementary Data. All new compounds were unambiguously characterized by ^{1}H and ^{13}C NMR, FT-IR and high resolution mass spectrometry (Supplementary Figs. S1-S9). The purity of the synthesized monofunctional Pt(II) complexes **Trz-Oxa** and **Ph-glu-Oxa** was confirmed to be >96% by analytical HPLC and the analysis results were presented in Supplementary Data (Figs. S10-S11). The water solubility of the complexes was also assessed and compared to the clinical drugs in Table 1 (see also Table S1) (see Scheme 2).

2.2. Anticancer activity in different tumor and oxaliplatin-resistant CRC cell lines

The anticancer activities of the synthesized monofunctional Pt(II) complexes were tested against several different cancer cell lines, namely, the human normal bronchial epithelial cells: BEAS-2B-CM, the human liver cancer cells: HePG2, the human melanoma cancer cells: Mel-RM. Especially we compared their actitivies in the oxaliplatin-sensitive CRC cells: HT29 and the established highly oxaliplatin-resistant HT29/Oxa cells. As summarized in Table 1, in all tested cell lines, including the normal bronchial epithelial BEAS-2B-CM cells, cisplatin exhibited stronger cytotoxicity than oxaliplatin except human colorectal cancer HT29 cells in which oxaliplatin showed more sensitivity than its predecessor cisplatin [16]. From the assay result we observed that cisplatin also showed moderate cross-resistance to this particular cell line HT29/Oxa, although 6-fold lower than oxaliplatin, with a resistance factor of 9.34. This result may reflect that cisplatin is partially sharing similar resistance mechanism with oxaliplatin [17]. Compared to cisplatin and oxaliplatin, the newly designed monofunctional Pt(II) complexes **Trz-Oxa** and **Ph-glu-Oxa**, however, exhibited low cytotoxicity against the normal cell lines indicating their improved selectivity between normal and carcinoma cells. Remarkably, the complex **Ph-glu-Oxa** with a bulky (1,4-disubstituted) triazole ligand showed almost no resistance against this oxaliplatin-resistant CRC cell line (RI = 1.15 vs. 53.83 for Oxa, Table 1).

2.3. In vivo efficacy of Ph-glu-Oxa versus oxaliplatin and cellular drug accumulation

Next, we explored if **Ph-glu-Oxa** could reverse the resistance of HT29/Oxa to oxaliplatin *in vivo*. We conducted the efficacy comparison study between **Ph-glu-Oxa** and oxaliplatin by using HT29/Oxa xenograft model. To understand the safety profile of the test molecule, we first finished a pre-test and a dose escalating experiment to determine the maximum tolerated dose of **Ph-glu-Oxa** by following the similar process of oxaliplatin MTD study according to our previous research [18]. Based on the maximum tolerated dose results we obtained for oxaliplatin in the xenograft mice (10.0 mg/kg), **Ph-glu-Oxa** showed an improved animal tolerance compared to oxaliplatin (MTD: 28.8 mpk vs 10 mpk, Table S2 and Fig. S12). For comparison reason, we applied a

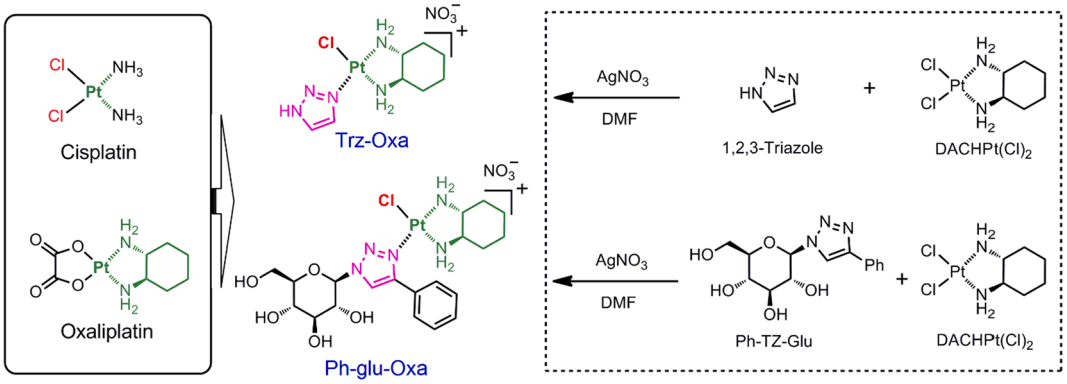

Scheme 1. Design concept and chemical structures of the monofunctional cationic Pt(II) complexes containing the same chiral DACH chelating ligand with oxaliplatin.

Table 1
Cytotoxicity of the monofunctional Pt(II) complexes against human normal, tumoral and oxaliplatin-resistant CRC cell lines.[a]

IC_{50} (μM)	BEAS-2B-CM	HepG2	Mel-RM	HT29	HT29/Oxa	Resistant Index (RI)[b]	Solubility (mg/mL)
Oxa	12.54 ± 1.52	45.19 ± 3.77	21.14 ± 2.01	6.23 ± 1.12	335.34 ± 6.33	53.83	6.16
Cis	7.89 ± 0.52	9.90 ± 0.92	4.72 ± 0.55	26.62 ± 2.03	248.62 ± 5.57	9.34	1.03
Trz-Oxa	>200	>200	>200	39.63 ± 2.82	155.22 ± 4.88	3.92	43.45
Ph-glu-Oxa	>200	40.10 ± 3.88	22.56 ± 1.99	9.77 ± 0.72	11.22 ± 1.00	1.15	19.14
1,2,3-Triazole	>200	>200	>200	>200	>200	/	/
Ph-TZ-Glu	>200	>200	>200	>200	>200	/	/

[a] Cell culture and MTT assay details are provided in Experimental Section. IC_{50} data are presented as means ± S.E.M from MTT assay for 72 h.
[b] Resistance index (RI) is the ratio of the IC_{50} value for the resistant cell line to the IC_{50} value for the parental cell line.

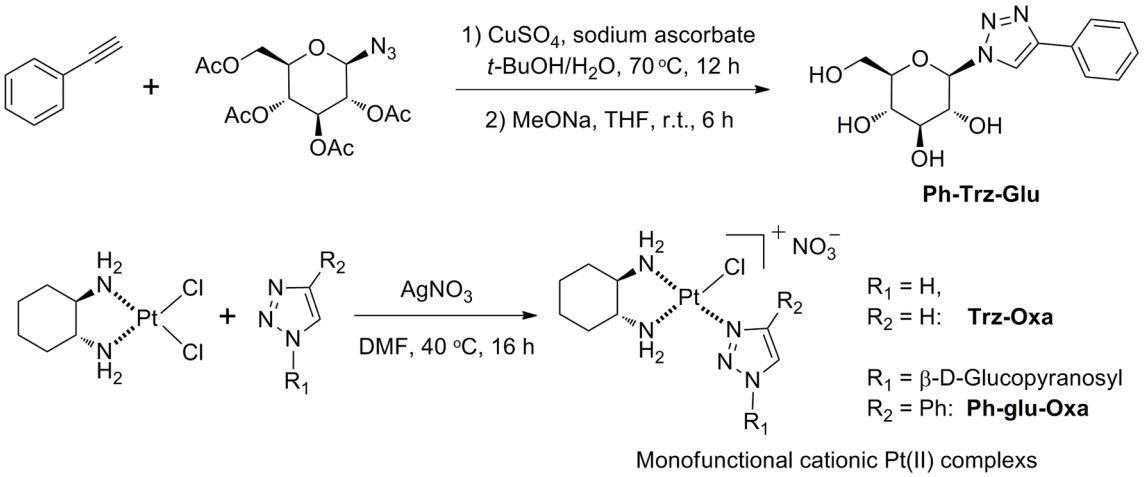

Scheme 2. Synthetic route of the monofunctional cationic Pt(II) complexes derived from triazole and glycoconjugated phenyltriazole containing chiral DACH chelating ligand.

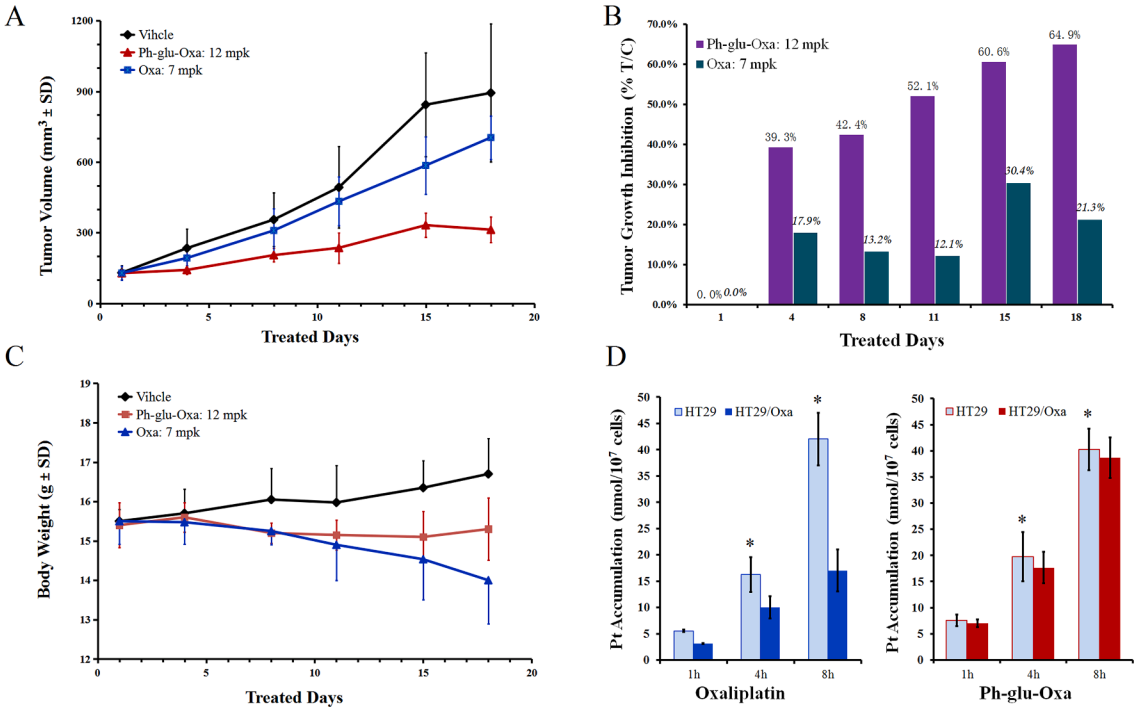

Fig. 1. (A) Tumor growth records with a 1/5/9 three injection treatment of oxaliplatin and Ph-glu-Oxa in HT29/Oxa xenograft model. (B) The tumor growth inhibition rate for both oxaliplatin and Ph-glu-Oxa treated mice (T/C ratio, the ratio of tumor volume in control versus treated mice at a specified time). The *p* value for %T/C of both oxaliplatin and Ph-glu-Oxa in was 0.01–0.003. (C) Body weight records from the efficacy study treated with 7 mpk oxaliplatin and 12 mpk of Ph-glu-Oxa. (D) Intracellular platinum accumulation in normal HT29 and oxaliplatin resistance HT29/Oxa cells after treatment with 40 μM of each oxaliplatin and Ph-glu-Oxa for 1, 4 and 8 h. *$P < 0.05$ compared to oxaliplatin treatment.

dosage of 70% of the MTD for oxaliplatin (7.0 mpk) and an equimolar dosage for **Ph-glu-Oxa** (12.0 mpk) in a schedule of three injections on days 1, 5 and 9, and the clinical and physiological observations were recorded for 18 days after the first injection. For details, BALB/c nude mice (4–5 weeks old) were obtained from Vital River (Beijing, China). HT29/Oxa cells (0.1 mL of 1.0×10^8) were transplanted subcutaneously into the right flank in each mouse. Drug administration were started after the tumor volume reached 100–200 mm^3 via i.v. tail vein injection at a dose of 7 mpk for oxaliplatin and 12 mpk for **Ph-glu-Oxa** with a control group of animals injected with PBS (n = 7). Oxaliplatin and **Ph-glu-Oxa** were administered on days 1, 5, 9 and tumor volume and body weight of the animals were measured in a 2–3 day basis and the data were recorded for another 10 days after the final injection. The mice were housed in pathogen-free conditions and National Institutes of Health guide for the care and use of laboratory animals was followed. All animal experiments were performed following a protocol approved by the Ethics Committees of Gudui BioPharma Technology Inc.

According to our previous *in vivo* study results using the same treatment dosage of oxaliplatin in HT29 xenograft model [18], the sensitivity of the HT29/Oxa derived tumors to oxaliplatin was notably decreased in the current resistance model (Fig. 1A). Compared to oxaliplatin, **Ph-glu-Oxa** exhibited significant sensitivity against HT29/Oxa tumors, with an increased tumor growth inhibition rate as illustrated in Fig. 1B (64.9% of highest %T/C vs 30.4% for oxaliplatin). Toxicity indicated by animal tolerability was also found to be more negligible for **Ph-glu-Oxa** than the clinical drug oxaliplatin (Fig. 1C). Furthermore, efficacy differences of oxaliplatin and **Ph-glu-Oxa** observed from the *in vivo* study were directly correlated with their intracellular drug concentrations respectively in the parental and resistance HT29/Oxa cell lines tested for both drugs (Fig. 1D). The intracellular total drug concentration was measured by Inductively Coupled Plasma Mass Spectrometry (ICP-MS) to determine the drug uptake differences between oxaliplatin and **Ph-glu-Oxa** respectively in HT29 and HT29/Oxa cell lines. As summarized in Fig. 1D, the intracellular accumulation of oxaliplatin in HT29/Oxa cells was significantly reduced compared with non-resistance HT29 cells. However, **Ph-glu-Oxa** maintained the same level of intracellular drug concentrations in both cell lines. The significant difference between oxaliplatin and **Ph-glu-Oxa** in intracellular platinum accumulation in HT29/Oxa cell lines (e.g. after 8 h incubation, 17.00 nmol for Oxa vs 38.66 nmol for Ph-glu-Oxa, Fig. 1D) is indicative evidence of the acquired resistance of CRC to oxaliplatin but no resistance to **Ph-glu-Oxa**.

2.4. Ciricular dichroism analysis

To explore the intrinsic DNA-damaging activity of the monofunctional platinum(II) complex, we first evaluated a time dependent DNA conformational changes induced by **Ph-glu-Oxa** using circular dichroism (CD) analysis. CD spectra of hsDNA in the absence or presence of the Pt(II) complexes were studied by treating **Ph-glu-Oxa** with hsDNA in different molar ratios for 12, 24, 48 and 72 h with comparison to oxaliplatin. The spectrum of the drug-only as well as the CD buffer alone were subtracted from the spectrum of the sample tests. The positive band at ~275 nm is due to base stacking, while helicity is responsible for the negative band at ~245 nm, which is characteristic of DNA in right-handed B form [19]. As shown in Fig. 2A, signifificant decrease in ellipticity on positive bands with a slight red shift, and a slight hypochromism on the negative bands were observed in a concentration- and time-dependent manner for **Ph-glu-Oxa** treated hsDNA. Such a CD pattern is an indication of B-form DNA conformational change induced by **Ph-glu-Oxa**, however the B to Z conformational conversion was not observed even at a higher concentration of the complex and prolonged incubation treatment (see Fig. S13). Overall, the CD pattern changes for both oxaliplatin and the monofunctional Pt(II) complex were similar except **Ph-glu-Oxa** may cause more significant decreases on positive band ellipticity than oxaliplatin indicating **Ph-glu-Oxa** is able to results in more deformation of the base stacking and helix unwinding, and eventually leads to the loss of DNA helicity.

2.5. Competitive ethidium bromide (EB) fluorescence quenching

As a DNA intercalator, EB binds with DNA minor groove and intercalates into base pairs of the DNA with no sequence preferences [20]. When Pt(II) complex interacts with EB-bound DNA, the structure of DNA will be purterbated or ruptured which results in a loss of EB fluorescence intensity [21]. As shown in Fig. 2B, the fluorescence emission intensity of EB at about 610 nm (λex = 522 nm) concentration-dependently decreases during titration of the EB-hsDNA system with **Ph-glu-Oxa**,

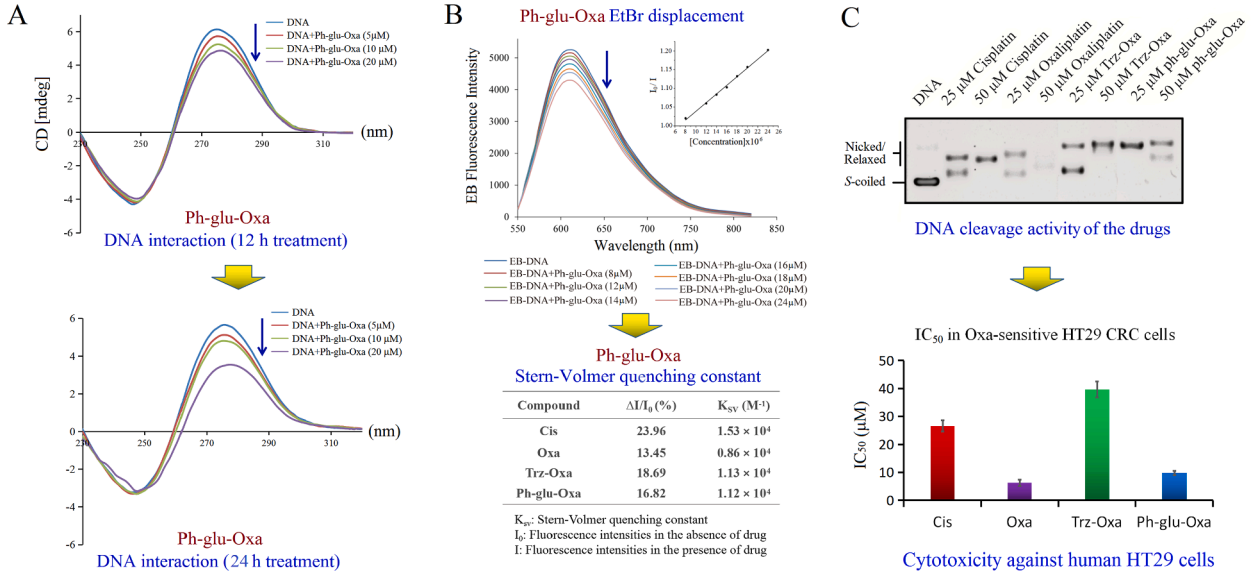

Fig. 2. (A) The circular dichroism spectra of hsDNA (1 μM) upon the varying concentrations of Ph-glu-Oxa after incubation at 37 °C for 12 and 24 h. (B) Fluorescence quenching spectra of EB-DNA titrated by increasing amounts of Ph-glu-Oxa. Inset: plot of [I_0/I] versus [Drug Concentration] (Upper). The Stern-Volmer constants (Ksv) value of cisplatin, oxaliplatin, Trz-Oxa and Ph-glu-Oxa (Lower) calculated from the Stern-Volmer equation (see SI Table S1). (C) Agarose gel electrophoresis of pBR322 plasmid DNA incubated with Pt(II) complexes in 5 mM Tris–HCl/50 mM NaCl buffer at 37 °C for 48 h. And the corresponding MTT assay results of the complexes against human HT29 cells (Lower).

indicating the partial removal of EB from DNA molecules due to the interaction of the Pt(II) complex with DNA. The inset of Fig. 2B shows the Stern-Volmer plot suggesting that the fluorescence quenching is ruled by the linear Stern-Volmer equation. The quenching constant (Ksv) data was summarized in the table underneath the fluorescence spectra. Comparison of the Ksv value for **Trz-Oxa** and **Ph-glu-Oxa** with cisplatin and oxaliplatin, both the DNA modification power of the monofunctional Pt(II) complexes seems falling between these two clinical drugs. To further confirm that if the chelating ligand (Triazole and Ph-TZ-Glu) themselves may also contribute to DNA denaturing, we also tested both compounds for EB-DNA quenching under the same condition. The results were provided in the Supplementary Data (Figs. S14-S15) which showed that triazole did not affect the EB-DNA complex at all, however, the bulky 1-glycosyl-4-phenyl triazole ligand exhibited weak perturbation to the EB-bound DNA with a small Ksv value of 0.47 $\times$ 10^4 (M^{-1}) (Table S3). Although both the ligands themselves did not show any cytotoxicity against the normal and tumoral cells (Table 1), this result indirectly supports the design concept of installing a bulkier chelating ligand into the Pt(II) complex that may contribute to more efficient DNA binding and denaturing as we have described in the introduction section.

2.6. Plasmid DNA cleavage

Effect of the monofunctional Pt(II) complexes **Trz-Oxa** and **Ph-glu-Oxa** (25–50 μM) on the pBR322 DNA cleavage was studied using agarose gel electrophoresis and compared with cisplatin and oxaliplatin. As shown in Fig. 2C, the electrophoretogram shows that all Pt(II) complexes were able to cleave the DNA by converting supercoiled circular DNA to nicked and/or relaxed DNA as indicated by band disappearance of the supercoiled DNA and band intensification of nicked/relaxed circular DNA. For both bifunctional clinical drugs: cisplatin and oxaliplatin, DNA cleavage pattern changes dramatically with the increase of drug concentrations (25–50 μM). Compared to cisplatin, a pronounced DNA cleavage and more formation of shorter DNA pieces were observed which evidenced by the disappearance of both supercoiled plasmid and the nicked DNA bands for 50 μM oxaliplatin incubation. Compared to cisplatin and oxaliplatin, both **Trz-Oxa** and **Ph-glu-Oxa** showed further difference in electrophoretogram bands pattern indicating that the monofunctional Pt(II) complexes were involved in different DNA-interaction mode compared to the bidentate clinical drugs. Furthermore, the results revealed that the DNA cleavage activity is sensitive to the variation of the ligand types between **Trz-Oxa** and **Ph-glu-Oxa**: at the low concentration (e.g. 25 μM), **Ph-glu-Oxa** yielded more nicked DNA products than **Trz-Oxa**, while under high concentration drug treatment (50 μM), **Ph-glu-Oxa** revealed an extensive DNA degradations as the appearance of a discernible linear DNA band in addition to the nicked DNA product. These results were correlated with the cytotoxic effect of each complex evaluated in the human HT29 CRC cell lines (Fig. 2C).

2.7. AFM imaging study on Ph-glu-Oxa/DNA interaction

Literatures have reported that the DNA topographic changes from cisplatin and oxaliplatin binding can be visualized using atomic force microscopy [22-24]. Fig. 3A shows the typical AFM images of the non-

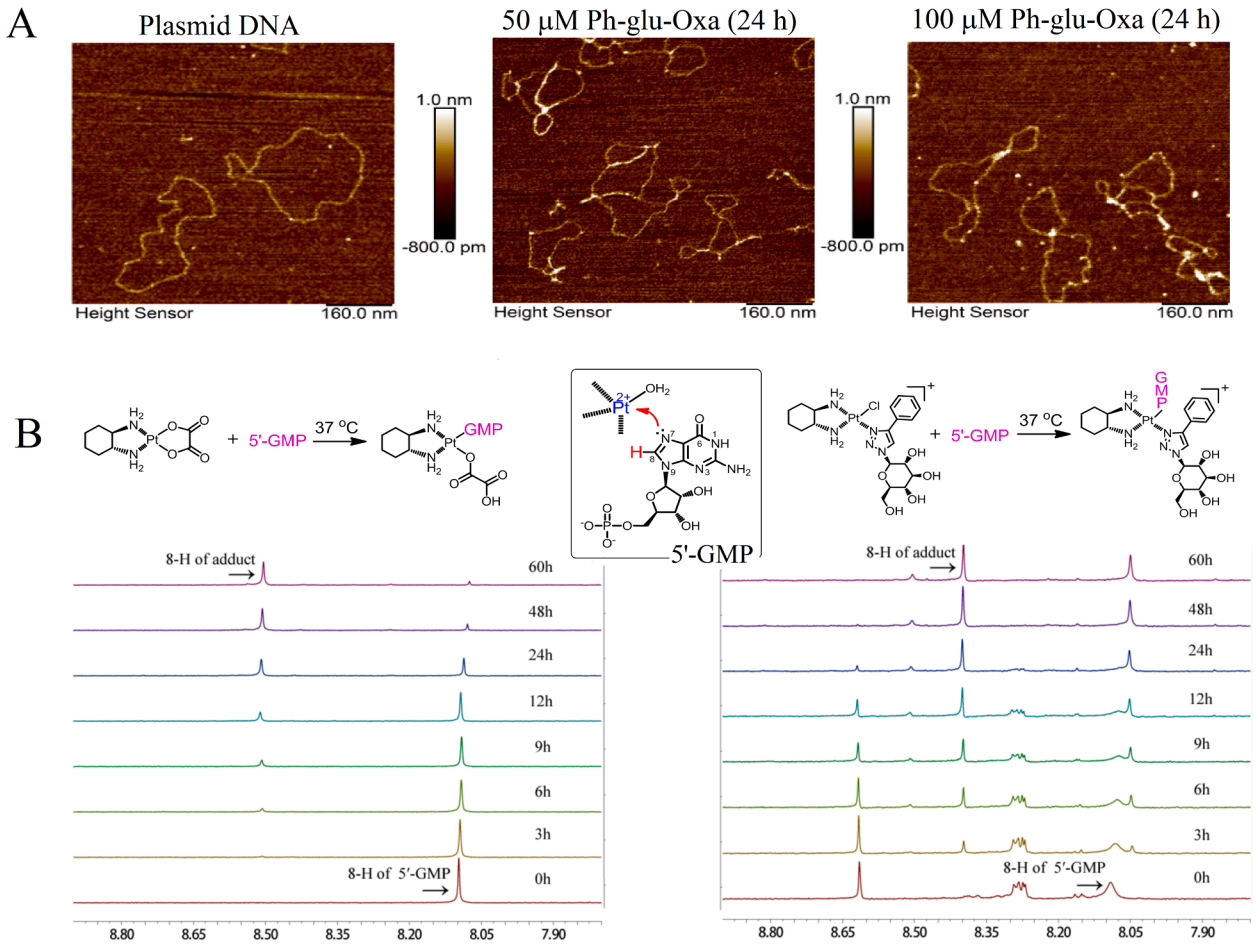

Fig. 3. (A) AFM topographic imaging analysis of the interaction of Ph-glu-Oxa with pBR322 plasmid DNA incubated with increasing amounts of the Pt(II) complex. (B) ^{1}H NMR spectra of the reaction kinetics of oxaliplatin and Ph-glu-Oxa with 5′-GMP (1:1) in D_2O in the presence of 5 mM of NaCl at 37 °C.

treated and damaged pBR322 plasmid DNA incubated with increasing amounts of **Ph-glu-Oxa**. After incubation with 50 μM of Ph-glu-Oxa for 24 h, the circle opening, micro-loop formation, DNA kinks induction, and the length shortening of the DNA which ascribed to local denaturation and helix unwinding by Pt-DNA linkages were observed. Increase of the drug concentration to 100 μM, more profound DNA damages represented by increased micro-kinks and interhelix bridges have been visualized. Based on these AFM analysis results, it can be concluded that both the DNA unwinding and local denaturation caused by platination of the monofunctional Pt(II) complex **Ph-glu-Oxa** is concentration and time dependent process (see Fig. S16 for time-dependent results). This is similar with the reported oxaliplatin mediated DNA-denaturing process [25] and supporting the *in vivo* efficacy results of **Ph-glu-Oxa** in CRC xenograft model.

2.8. DNA reactivity investigation

The intrinsic DNA-adduct formation capacity of the Pt(II) complex can be determined by the relative reactivity analysis of **Ph-glu-Oxa** with guanosine-5′-phosphate (5′-GMP). We used NMR spectroscopy to monitor reactions of the Pt(II) complexes with 5′-GMP to compare the differences of our monofunctional complex and cis- and oxaliplatin. To mimic the intracellular environment, 5 mM of NaCl and deuterated water were used with 1 equimolar of 5′-GMP per Pt(II) complex. The reactions were carried out at 37 °C. The reaction of each Pt(II) complex with 5′-GMP was monitored using ^{1}H NMR spectroscopy to observe the disappearance of the H8 signal of the 5′-GMP at 8.04 ppm and the appearance of a new H8 signal from the corresponding GMP-N7-Pt(II) adduct at 0.5–1.0 ppm downfield of the unreacted 5′-GMP. As shown in Fig. 3B and Fig S17, **Ph-glu-Oxa**, the newly synthesized monofunctional Pt(II) complex with a sterically hindered disubstituted triazole ligand, exhibited a similar reaction kinetics towards 5′-GMP with cisplatin rather than the parental compound oxaliplatin. The reaction half time of **Ph-glu-Oxa** was recorded as 7.30 h ($T_{1/2}$ = 5.25 h and 25.0 h for cisplatin and oxaliplatin, Fig. S14). Similar to other reported monofunctional cicplatin derivatives [9,26], this result revealed that the steric hindrance itself may not be the key interference factor for the Pt (II) electrophilic center against guanosine nucleophile, but the π-acceptor effect of the Ph-TZ-Glu ligand may play an important role to accelerate the reactivity toward 5′-GMP through π-π stacking interaction (for entire NMR spectra, see Figs. S18-S19).

2.9. GSH reactivity investigation

From the cellular drug accumulation study results described in Section 2.3, the enhanced anti-tumor efficacy of **Ph-glu-Oxa** in oxaliplatin-resistant CRC treatment can be at least attributed to the decreased drug efflux of the drug molecule. Previous studies demonstrated that tolerance and resistance of oxaliplatin is often accompanied with elevated cellular glutathione (GSH) and glutathione S-transferase, and consequently, detoxification of oxaliplatin by intracellular formation of platinum-glutathione adducts (GS–Oxa). The promoted cellular efflux of such adducts via glutathione S-conjugate export pump (GS-X pump) is responsible for decreased accumulation of oxaliplatin and results in drug resistance [14,27,28] To verify whether the steric hindrance of the Ph-TZ-Glu ligand may potentially contribute to inactivation of **Ph-glu-Oxa** against GSH molecule, we conducted a high-resolution electrospray ionization mass spectrometry study (HR-ESI-MS). To ensure there is

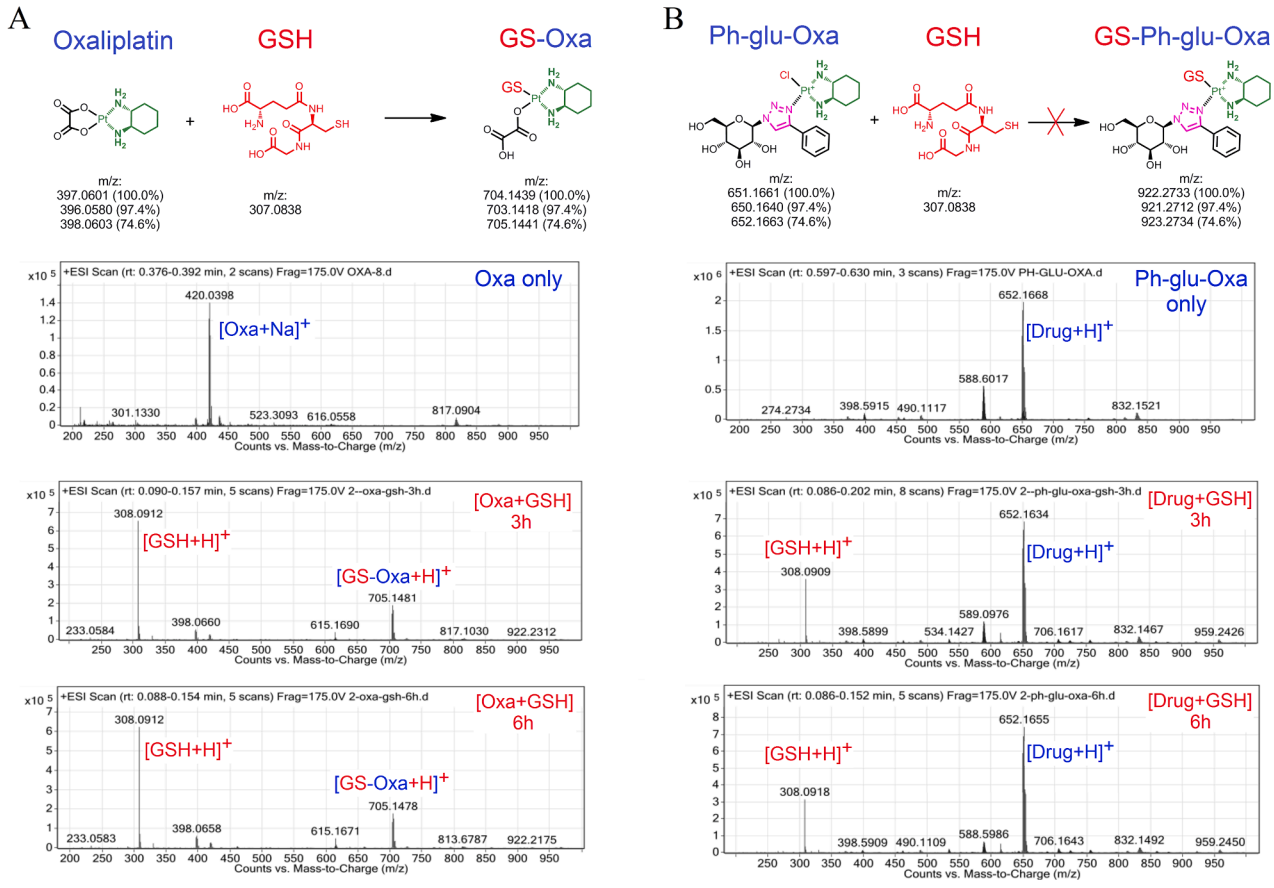

Fig. 4. (A) High-resolution electrospray ionization mass (positive mode) determination on GSH-conjugation reaction of oxaliplatin to afford oxaliplatin-GSH adduct at *m/z* 705 relative to $[GS\text{-}Oxa + H]^{+}$. (B) No GSH-conjugate formation was observed between Ph-glu-Oxa and GSH up to 6 h. Experiments were carried out using a 1:1.2 M ratio mixture of the Pt(II) complexes and GSH in water for up to 24 h incubation at 25 °C.

enough GSH monomer that is the most active nucleophile in the reaction system, we used a 1:1.2 M ratio mixture of the Pt(II) complex and GSH in water solution using the metal sensitive positive ion mode. As shown in Fig. 4A, the base and targeted molecular peaks in the mass spectrum is assigned for oxaliplatin/GSH reaction system as follows: 1) the protonated GSH ion $[GSH + H]^+$ at *m/z* 308; 2) the sodium adduct of Oxa ion $[Oxa + Na]^+$ at *m/z* 420; 3) the GSH adduct of Oxa ion $[GS\text{-}Oxa + H]^+$ at *m/z* 705. Accordingly, for the **Ph-glu-Oxa**/GSH reaction system, the assignment were: 1) the protonated GSH ion $[GSH + H]^+$ at *m/z* 308; 2) the protonated **Ph-glu-Oxa** (drug) ion $[Drug + H]^+$ at *m/z* 652; 3) the GSH adduct of **Ph-glu-Oxa** ion $[GS\text{-}Drug + H]^+$ at *m/z* 923 (Fig. 4B).

As seen in Fig. 4A, the oxaliplatin-GSH adduct at *m/z* 705 relative to that of $[GS\text{-}Oxa + H]^+$ is clearly observed after 3 h incubation with GSH and the completion of the reaction is indicated by the consumption of the oxaliplatin starting material and formation of the $[GS\text{-}Oxa + 1]^+$ signal as the mono-GSH product. The dominant product from the current study shows that GSH reacts with oxaliplatin prior to the dissociation of the oxalate ligand. The similar result has been observed in the previous report in a 2:1 mixture of GSH and oxaliplatin [11]. In contrast, for the **Ph-glu-Oxa**/GSH system, the desired [GS-Ph-glu-Oxa] adduct has not been observed under the same condition up to 6 h incubation (Fig. 4B). This is indicative of the fact that there was a significant difference between oxaliplatin and the newly synthesized monofunctional Pt(II) complex in terms of the reaction mode with GSH. Apparently, the reaction of **Ph-glu-Oxa** with GSH proceeds extremely slowly as a 24 h incubation result showed only a trace amount of the GSH adduct of **Ph-glu-Oxa** relative to $[GS\text{-}Drug + H]^+$ at *m/z* 923 (Fig. S20). The results suggest that the steric hindrance of the Ph-TZ-Glu ligand might be an important factor affecting the reaction mode with the bulk aliphatic tripeptide GSH. Considering the high reactivity of **Ph-glu-Oxa** towards 5′-GMP, the HR-ESI-MS results also revealed that the influence of both the steric hindrance as well as the π-conjugated structural characteristic of Ph-TZ-Glu ligand may play key roles to maintain the cytotoxicity of the Pt(II) complex while diminish the detoxification effect of the sulfur-containing molecules.

2.10. Molecular dynamics study of DNA-binding mode

To understand the possible binding interaction of **Ph-glu-Oxa** with DNA, we conducted a molecular dynamics simulation (MD) study according to the reported X-ray crystal structure of pyriplatin $[Pt(NH_3)_2(py)]^{2+}$ monofunctional Pt(II) complex with a DNA dodecamer duplex [29]. Simulations were carried out using YASARA molecular simulation program (YASARA Biosciences. YASARA: Yet another scientific artificial reality application. http://www.yasara.org/). Based on the DNA-pyriplatin 3D structure (PDB ID: 3CO3), the native ligand of bound-pyriplatin was replaced with **Ph-glu-Oxa** and a short (30 ns) time scale molecular dynamics simulation was performed.

As depicted in Fig. 5A–B, by platinum coordination with the N7 of guanine base, **Ph-glu-Oxa** was able to adopt a standing-up position in the major groove alongside the helix axis (Fig. 5B). MD result revealed that, due to stereo hindrance of both DACH and glycoconjugated phenyltriazole, the single base binding of **Ph-glu-Oxa** may potentially cause Watson-Crick hydrogen bonding breakdown and more significant DNA duplex unwinding (Fig. 5A vs 5B). In addition to the intrinsic reactivity toward 5′-GMP, the MD simulation result, from another perspective, reveals that the stronger cytotoxicity of **Ph-glu-Oxa** may originate from its strong DNA transcription inhibitory profiles. On the other hand, the retarded reactivity against the sulfur-containing nucleophile, such as those associated with cellular resistance mechanisms, like GSH, makes an important feature of **Ph-glu-Oxa**.

3. Conclusion

Based on the unique DACH ligated structural characteristic and biological properties of oxaliplatin, we have designed and synthesized a cationic monofunctional DACH-Pt(II) complex **Ph-glu-Oxa**, which contains a sterically bulky 1-glycosyl-4-phenyl-1,2,3-triazole chelating ligand (Ph-TZ-Glu). In vitro assay demonstrated that **Ph-glu-Oxa** was potently cytotoxic against both the oxaliplatin sensitive and resistant CRC cells with diminished resistance index. Study results on kinetic reactivity analysis with 5′-GMP revealed a greater electrophilic reactivity of the cationic Pt(II) complex towards the nucleotide compared to the parental oxaliplatin. The $T_{1/2}$ for mono GMP-adduct formation was recorded as 7.3 h versus 25.0 h for oxaliplatin demonstrating the DNA binding potential of the complex was significantly increased. Other investigation results including plasmid DNA cleavage, circular dichroism-mediated DNA deformation as well as EtBr fluorescence quenching and AFM based DNA denaturation analyses were also in agreement in supporting that the newly synthesized monofunctional Pt(II) complex is intrinsically a favorable DNA interactor. Most importantly, **Ph-glu-Oxa** has been found to be highly efficacious in oxaliplatin-resistant CRC xenograft model, which is associated with high intracellular accumulation of the drug in oxaliplatin-resistant HT29/Oxa cell lines.

The molecular basis of the anti-resistance profile for **Ph-glu-Oxa**, in the current study, was elucidated through the investigation of the susceptibility of the complex to glutathione (GSH)-mediated detoxification. Compared to oxaliplatin, **Ph-glu-Oxa** was proved to be very inert against GSH-mediated platinum-conjugation. Reaction of **Ph-glu-Oxa** with GSH proceeds extremely slowly in contrast to the GMP-mediated neucleophilic addition. The significant difference between oxaliplatin and **Ph-glu-Oxa** in GSH-conjugation capability may attribute to the designer molecular structure of **Ph-glu-Oxa**. That is, the steric

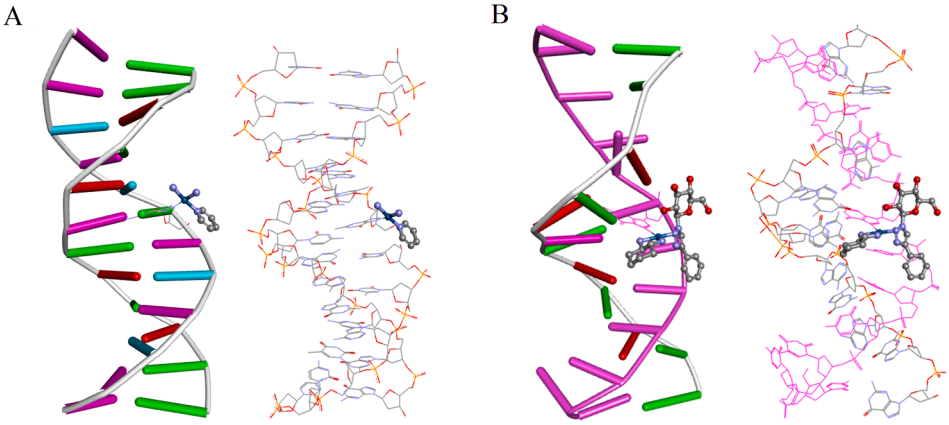

Fig. 5. (A) Crystall structure of pyriplatin $[Pt(NH_3)_2(py)]^{2+}$ monofunctional Pt(II) complex with a DNA dodecamer duplex (PDB ID: 3CO3). (B) Calculated DNA-binding conformation of Ph-glu-Oxa with a DNA dodecamer duplex from MD simulation study.

hindrance of the Ph-TZ-Glu ligand might prevent the nucleophilic addition of the complex against bulky tripeptide GSH nucleophile, while the π-acceptor effect of the Ph-TZ-Glu ligand may help altering the reactivity of the drug molecule against the DNA base pairs. Accordingly, the insusceptibility of **Ph-glu-Oxa** to GSH-mediated detoxification may play a key role in maintaining cytotoxicity and to counteract oxaliplatin-induced drug resistance. Nevertheless, additional pharmacological targets cannot be excluded, and more studies are necessary to deeply elucidate their mechanism of action.

4. Experimental methods

4.1. Preparation of the monofunctional Pt(II) complexes: *Trz-Oxa*

[Pt(DACH)Cl_2] (100.00 mg, 0.26 mmol) was dissolved in DMF (5.0 mL) and treated with silver nitrate (44.80 mg, 0.26 mmol) at 40 °C for 16 h under protection from light. The resulting AgCl precipitate was discarded by filtration. Triazole (13.75 μL, 16.40 mg, 0.24 mmol) was added to the filtrate and the solution was stirred at 40 °C for 16 h under dark. Diethyl ether (50.0 mL) was added to the solution to give a white precipitate which was collected by filtration. The precipitate was dissolved in methanol (3.0 mL) and the insoluble oxaliplatin was filtered and discarded. Diethyl ether (20.00 mL) was added to the filtrate to give a white precipitate which was collected by filtration. The final product was washed with diethyl ether, dried in vacuum to afford a white solid. (92.35 mg, 73.69% yield). ^{1}H NMR (600 MHz, DMSO-d_6) δ 8.43 (d, J = 0.9 Hz, 1H), 8.18 (d, J = 1.2 Hz, 1H), 6.17 (d, J = 9.6 Hz, 1H), 6.02 (d, J = 9.0 Hz, 1H), 5.81–5.75 (m, 1H), 5.57–5.52 (m, 1H), 2.26–2.22 (m, 2H), 1.94–1.88 (m, 2H), 1.49 (s, 2H), 1.33–1.28 (m, 2H), 1.02 (t, J = 9.7 Hz, 2H); ^{13}C NMR (150 MHz, DMSO-d_6) δ 133.32, 125.52, 62.20, 61.91, 31.45, 31.26, 24.02, 23.87; IR: Vmax. KBr (cm^{-1}): 3198, 3102, 2939, 2863, 1322, 1165, 1031, 921, 794, 512, 439; HRMS: Calcd. For $C_8H_{17}ClN_5Pt$ (M+H) $^+$: 414.0816, found 414.0814.

4.2. Preparation of the monofunctional Pt(II) complexes: *Ph-glu-Oxa*

1-β-*D*-glucopyranosyl-4-phenyl-1H-1,2,3-triazole (Ph-Trz-Glu) was synthesized with a slightly modified procedure reported in reference [30]. To a solution of ethynylbenzene (100.00 mg, 0.98 mmol) and 2,3,4,6-tetra-O-acetyl-β-*D*-glucopyranosyl azide (402.18 mg, 1.08 mmol) in 8.0 mL of *t*-BuOH/H_2O (v/v: 1:1), $CuSO_4{\cdot}5H_2O$ (125.22 mg, 0.49 mmol), sodium ascorbate (381.55 mg, 1.96 mmol) were added and the reaction mixture was heated at 70 °C for 12 h. After cooling to the room temperature, distilled water was added and the reaction mixture was extracted with CH_2Cl_2. The obtained organic phase was dried over anhydrous Na_2SO_4 and concentrated under reduced pressure. The crude product was purified by column chromatography using silica gel (PE: EA = 3:1) to afford 2,3,4,6-tetra-O-acetyl-β-*D*-glucopyranosyl-4-phenyl-1H-1,2,3-triazole as a colorless oil (384.17 mg, 82.50%). Deacetylation of the compound (300.00 mg, 0.63 mmol) was carried out using MeONa (7.05 mg, 0.13 mmol) in THF (6.00 mL) at room temperature for 6 h monitored by TLC. The crude product was purified by column chromatography using silica gel (DCM: MeOH = 10:1) to afford 1-β-*D*-glucopyranosyl-4-phenyl-1H-1,2,3-triazole as a white solid (146.08 mg, 75.50%). The structure and stereochemistry were characterized according to the literature. ^{1}H NMR (600 MHz, MeOD) δ 8.56 (s, 1H), 7.86–7.83 (m, 2H), 7.44 (t, J = 7.7 Hz, 2H), 7.35 (t, J = 7.4 Hz, 1H), 5.65 (d, J = 9.2 Hz, 1H), 3.96 (t, J = 9.1 Hz, 1H), 3.90 (dd, J = 12.3, 2.0 Hz, 1H), 3.74 (dd, J = 12.3, 5.5 Hz, 1H), 3.63–3.58 (m, 2H), 3.56–3.51 (m, 1H).

Following the same procedure as described for Trz-Oxa preparation, [Pt(DACH)Cl_2] (100.0 mg, 0.26 mmol) was dissolved in DMF (5.0 mL) and silver nitrate (44.80 mg, 0.26 mmol) was added and the mixture was stirred at 40 °C for 16 h under protection from light. The resulting AgCl precipitate was discarded by filtration. To the filtrate, Ph-Trz-Glu (72.90 mg, 0.24 mmol) was added, and the solution was stirred for 16 h at 40 °C. Diethyl ether (50.00 mL) was added to the solution to give a white precipitate which was collected by filtration. The precipitate was dissolved in methanol (3.0 mL) and the insoluble oxaliplatin was filtered and discarded. Diethyl ether (20.00 mL) was added to the filtrate to give a white precipitate as the desired product. The precipitate was washed with diethyl ether and dried under vacuum to afford the final product as a white solid. (116.35 mg, 61.84% yield) ^{1}H NMR (600 MHz, DMSO-d_6) δ 9.10 (s, 1H), 8.50 (d, J = 7.3 Hz, 2H), 7.52 (dt, J = 28.8, 7.3 Hz, 3H), 6.05 (d, J = 8.6 Hz, 1H), 6.00 (d, J = 9.9 Hz, 1H), 5.64 (d, J = 9.2 Hz, 1H), 5.60 (d, J = 5.8 Hz, 1H), 5.54 (t, J = 9.5 Hz, 1H), 5.44 (d, J = 4.7 Hz, 2H), 5.24 (d, J = 5.5 Hz, 1H), 4.71 (t, J = 5.7 Hz, 1H), 3.91–3.84 (m, 1H), 3.75–3.69 (m, 1H), 3.55–3.44 (m, 3H), 3.31–3.26 (m, 1H), 2.27 (s, 2H), 1.87 (dd, J = 24.9, 12.0 Hz, 2H), 1.47 (d, J = 7.4 Hz, 2H), 1.31 (d, J = 9.1 Hz, 2H), 1.01 (t, J = 10.0 Hz, 2H); ^{13}C NMR (150 MHz, DMSO-d_6) δ 129.33, 128.44, 128.14, 127.60, 126.29, 124.75 88.82, 80.30, 76.40, 71.74, 69.30, 62.34, 62.03, 60.58, 31.28, 30.96, 23.94, 23.91; IR: Vmax. KBr (cm^{-1}): 3200, 2887, 1669, 1632, 1394, 1282, 1100, 1068, 766, 696, 591, 507, 470; HRMS: Calcd. For $C_{20}H_{31}ClN_5O_5Pt$ (M+H) $^+$: 652.1657, found 652.1649.

4.3. Cell culture and establishment of oxaliplatin-resistant HT29 cell line

Human lung epithelial cell BEAS-2B and all three tumor cell lines, HepG2, Mel-RM and HT29 used in the present study were purchased from ATCC. HT29 cells were cultured in RPMI 1640 medium (High Glucose; Gibco, Invitrogen) supplemented with 10% fetal bovine serum (FBS; Gibco, Invitrogen) and 1% penicillin/streptomycin solution (Gibco, Invitrogen); BEAS-2B, HepG2 and Mel-RM cells were cultured in Dulbecco's modified Eagle's medium (DMEM 1x, High Glucose; Gibco, Invitrogen) with 10% fetal bovine serum and 100 U·mL^{-1} penicillin-streptomycin at 37 °C under a 5% CO_2 environment.

For establishment of stable Oxa-resistant cells, HT29 cells were exposed to an initial oxaliplatin concentration of 0.1 μM in culture medium supplemented with 10% fetal bovine serum and 1% penicillin-streptomycin at 37 °C under a 5% CO_2 environment. This treatment continued for 2 weeks with collection of the surviving cells. The surviving cells were then gradually exposed to higher concentration of oxaliplatin (0.5 μM, 1.0 μM, 2.0 μM, 5.0 μM) and repeat the surviving cell collection process. Cells were cultured with each concentrations of oxaliplatin for 4 weeks. The resultant subline proved stably resistant after 3 months growth in drug free medium.

4.4. Cell viability assay

The BEAS-2B-CM, HepG2, Mel-RM, HT29 and the oxaliplatin resistant HT29/Oxa cells were seeded at a density of 5000 cells per well in a flat bottomed 96-well using 100 μL of culture medium on day 0. On day one, cells were treated with increasing doses of the platinum complexes (0, 1, 5, 10, 50, 100, 250 and 500 μM) for 72 h. 100 μL of culture medium was removed. MTT (Sigma-Aldrich) was added to each well at the final concentration of 0.83 mg/mL and incubated for 4 h. Cells were lysed by MTT lysis buffer (15% SDS, 0.015 M HCl) and the uptake of MTT was measured at 490 nm using a multi-well-reading UV–Vis spectrometer. For each platinum complex, the rates of cell survival were expressed as the relative percentage of absorbance compared to control. Experiments were performed in five replicates (5 wells of the 96-well plate per experimental condition) and repeated for three times. In this MTT assay, 1 mM of Trz-Oxa, Ph-glu-Oxa and oxaliplatin were freshly prepared by using double-distilled water at room temperature and sonicated in water bath for 15 min.

4.5. In vivo efficacy study on oxaliplatin-resistant xenograft mice

BALB/c nude mice (4–5 weeks old) were obtained from Vital River (Beijing, China). 0.1 mL of 1.0 × 10^8 HT29/Oxa cells were transplanted subcutaneously into the right flank in each mouse. The mice were

housed in pathogen-free conditions until the tumor volume reached 100–200 mm^3. The maximum tolerated dose was confirmed to be 10 mpk for oxaliplatin following the similar process according to our previous research [15]. Oxaliplatin was administered via i.v. tail vein injection at a dose equal to 70% of the MTD (7.0 mpk). The equimolar of Ph-glu-Oxa (12 mpk) was applied for comparison of the efficacy and drug resistance reversibility of the two drugs. Oxaliplatin and Ph-glu-Oxa were administered on days 1, 5, 9 and tumor volume and body weight of the animals were measured in a 3–4 day basis and the data were recorded for another 10 days after the final injection. National Institutes of Health guide for the care and use of laboratory animals was followed and these animal experiments were performed following a protocol approved by the Ethics Committees of Tianjin University.

4.6. Circular dichroism analysis

Circular dichroism spectra were determined at 37 °C using a Jasco J-815 spectropolarimeter equipped with a Jasco PTC-423 S Peltier temperature controller. Various concentrations of Pt(II) complexes were premixed with hsDNA in Tris–HCl buffer (50 mM Tris–HCl, 50 mM NaCl, pH = 7.2) at a constant temperature of 37 °C for 24 h. A 1 cm path quartz cell was used for each CD measurements and recorded the data after averaging over 3 accumulations with a scan speed of 100 nm min^{-1}. The scanning region was 220–320 nm.

4.7. Fluorescence quenching analysis

Quenching of the fluorescence of DNA-intercalated ethidium bromide (EB) was performed to investigate the DNA-binding profiles of the Pt(II) complexes. The EB-DNA mixture (1 μM EB and 1 μM hsDNA) was pretreated at room temperature for 0.5 h in Tris–HCl buffer (50 mM Tris–HCl, 50 mM NaCl, pH = 7.2). Emission spectra were obtained in the region between 550 and 850 nm at room temperature with a fixed excitation wavelength of 522 nm during the addition of the increasing concentrations of the Pt(II) complexes. Fluorescence spectra of solutions containing EB–DNA-bound mixtures with various concentrations of the complexes were acquired after 1 h of incubation. The quenching ability can be analyzed according to the Stern-Volmer equation.

$$I_0/I = 1 + K_{SV}[Q]$$

where I_0 and I are the fluorescence intensities in the absence and presence of the Pt(II) complexes. K_{SV} is the Stern-Volmer quenching constant and [Q] is the concentration of the compounds (quencher). The plots I_0/I versus the [Q] indicates a linear relationship of the data. The Ksv was obtained as the slope from the plots.

4.8. Reaction of Pt(II) complexes with GSH

The reaction between Pt(II) complex and GSH in a 1:1.2 M ratio was investigated in H_2O by ESI-MS. High-resolution mass spectrometry (HRMS) was performed on a Bruker MicroTOF spectrometer using positive ion mode (ESI+). The samples were analyzed by ESI-MS right after their preparation (0 h) and after 3 h, 6 h, 24 h of standing at room temperature.

4.9. Reaction of Pt(II) complexes with 5′-GMP

The reaction between Pt(II) complex and 5′-GMP was carried out in a 1:1 M ratio in deuterium oxide (contain 5 mM NaCl, pH = 6.70) at 37 °C. Samples were incubated for 3, 6, 9, 12, 24, 48 and 60 h. A series of ^1H NMR spectra for the reaction were recorded at appropriate times.

4.10. Atomic force microscopy

The pBR322 plasmid DNA (Thermo Fisher Scientific) at 1 ng/μL concentration was used for the experiments. Stock solutions (50 μM or 100 μM) of the complexes in deionized water were freshly prepared. AMF test solutions were prepared by diluting plasmid DNA and the Pt(II) complex stock solution with Tris-HCl buffer (10 mM $MgCl_2$, pH = 7.2) according to the designed concentrations. All samples were passed through 0.2 μm filters and the resulting solutions were incubated for 24 h at room temperature. AFM test samples were prepared by placing a drop (10 μL) of DNA solution or DNA − Pt complex solution onto freshly cleaved mica sheets (TED PELLA, INC. California, USA). After adsorption for 10 min at room temperature, the samples on mica surface were rinsed for 10 s with deionized water and dried under a stream of argon gas. AFM imaging was performed on atomic force microscope (Dimension icon Bruker, Germany). The images were obtained in air at room temperature on areas of 1 × 1 μm and operating in tapping mode at a rate of 1 Hz.

4.11. DNA cleavage analysis

The DNA cleavage property of Pt(II) complex was analyzed by concentration-dependent DNA cleavage agarose gel electrophoresis method. The DNA cleavage study of the complex was performed on 25 ng/μL of pBR322 DNA incubated at 37 °C for 48 h with increasing concentration of Pt(II) complex (25–50 μM) in aqueous buffer solution (5 mM Tris-HCl, 50 mM NaCl, pH = 7.2). After electrophoresis samples were photographed under UV light.

4.12. Cellular accumulation of platinum

The intracellular accumulation of platinum was measured in HT29 normal colon cancer cells and oxaliplatin-resistant HT29/Oxa cells to determine the differences between oxaliplatin and Ph-glu-Oxa. About 10 million HT29 and HT29/Oxa cells were treated with 40 μM oxaliplatin and Ph-glu-Oxa for 1 h, 4 h and 8 h, respectively, at 37 °C in a humidified 5% CO_2 incubator. After removing of the culture medium, the cells were washed three times with ice-cold PBS. After centrifugation for 5 min at 3000*g*, the cell pellets were homogenized using 1 M NaOH (1 mL) and diluted with 2% (v/v) HNO_3 (5 mL) for determining the whole cell platinum content. The homogenized samples were re-centrifuged for 10 min at 3000*g* and the supernatants were collected and ultrafiltered using Centrifree tubes (Amicon Inc, Beverly, MA, USA). The platinum contents were determined by ICP-MS. The instrument was calibrated using standard solutions containing 10, 50, 100, 500, and 1000 ppb platinum.

4.13. Statistical analysis

Differences between the samples were evaluated for statistical significance using Student's unpaired *t*-test. The level of significance was set at 5% with two-sided analysis. In vitro data from three different independent results were shown as mean ± SD.

Declaration of Competing Interest

The authors declare that they have no known competing financial interests or personal relationships that could have appeared to influence the work reported in this paper.

Acknowledgements

We would like to express our gratitude to all investigators who helped with providing materials and participated in this subject. This work was supported by the National Natural Science Foundation of China (No. 21772144) and the National Key Research & Development (R&D) Program of China (2020YFA0907903).

Appendix A. Supplementary material

Supplementary data to this article can be found online at https://doi.org/10.1016/j.bioorg.2021.104636.

References

[1] T. Alcindor, N. Beauger, Oxaliplatin: a review in the era of molecularly targeted therapy, Curr. Oncol. 18 (2011) 18–25.
[2] R.F. Ozols, S.D. Williams, Testicular cancer, Curr. Probl. Cancer 13 (1989) 285–335.
[3] J.M. Woynarowski, S. Faivre, M.C.S. Herzig, B. Arnett, W.G. Chapman, A. V. Trevino, E. Raymond, S.G. Chaney, A. Vaisman, M. Varchenko, P.E. Juniewicz, Oxaliplatin-induced damage of cellular DNA, Mol. Pharmacol. 58 (2000) 920–927.
[4] D.M. Kweekel, H. Gelderblom, H.J. Guchelaar, Pharmacology of oxaliplatin and the use of pharmacogenomics to individualize therapy, Cancer Treat. Rev. 31 (2005) 90–105.
[5] J.S. Tomlinson, W.R. Jarnagin, R.P. DeMatteo, Y. Fong, P. Kornprat, M. Gonen, N. Kemeny, M.F. Brennan, L.H. Blumgart, M. D'Angelica, Actual 10-year survival after resection of colorectal liver metastases defines cure, J. Clin. Oncol. 25 (2007) 4575–4580.
[6] N.F. Jensen, J. Stenvang, M.K. Beck, B. Hanakova, K.C. Belling, K.N. Do, B. Viuff, S. B. Nygard, R. Gupta, M.H. Rasmussen, L.S. Tarpgaard, T.P. Hansen, E. Budinska, P. Pfeiffer, F. Bosman, S. Tejpar, A. Roth, M. Delorenzi, C.L. Andersen, M.U. Romer, N. Brunner, J.M.A. Moreira, Establishment and characterization of models of chemotherapy resistance in colorectal cancer: towards a predictive signature of chemoresistance, Mol. Oncol. 9 (2015) 1169–1185.
[7] E. Martinez-Balibrea, A. Martinez-Cardus, A. Gines, V.R. de Porras, C. Moutinho, L. Layos, J.L. Manzano, C. Buges, S. Bystrup, M. Esteller, A. Abad, Tumor-related molecular mechanisms of oxaliplatin resistance, Mol. Cancer Ther. 14 (2015) 1767–1776.
[8] S. Ahmad, Platinum-DNA interactions and subsequent cellular processes controlling sensitivity to anticancer platinum complexes, Chem Biodivers. 7 (2010) 543–566.
[9] G.Y. Park, J.J. Wilson, Y. Song, S.J. Lippard, Phenanthriplatin, a monofunctional DNA-binding platinum anticancer drug candidate with unusual potency and cellular activity profile, Proc. Natl. Acad. Sci. U. S. A. 109 (2012) 11987–11992.
[10] J.D. Monroe, H.L. Hruska, H.K. Ruggles, K.M. Williams, M.E. Smith, Anti-cancer characteristics and ototoxicity of platinum(II) amine complexes with only one leaving ligand, PLoS ONE 13 (2018) e0192505.
[11] T. Shoeib, B.L. Sharp, Interactions of oxaliplatin with the cytoplasmic thiol containing ligand glutathione, Metallomics 4 (2012) 1308–1320.
[12] J. Reedijk, Why does cisplatin reach guanine-N7 with competing S-donor ligands available in the cell? Chem. Rev. 99 (1999) 2499–2510.
[13] S. Hector, W. Bolanowska-Higdon, J. Zdanowicz, S. Hitt, L. Pendyala, In vitro studies on the mechanisms of oxaliplatin resistance, Cancer Chemother. Pharmacol. 48 (2001) 398–406.
[14] Z. el-akawi, M. Abu-hadid, R. Perez, J. Glavy, J. Zdanowicz, P.J. Creaven, L. Pendyala, Altered glutathione metabolism in oxaliplatin resistant ovarian carcinoma cells, Cancer Lett. 105 (1996) 5–14.
[15] S. Cascinu, V. Catalano, L. Cordella, R. Labianca, P. Giordani, A.M. Baldelli, G. D. Beretta, E. Ubiali, G. Catalano, Neuroprotective effect of reduced glutathione on oxaliplatin-based chemotherapy in advanced colorectal cancer: a randomized, double-blind, placebo-controlled trial, J. Clin. Oncol. 20 (2002) 3478–3483.
[16] J.P. Armand, V. Boige, E. Raymond, K. Fizazi, S. Faivre, M. Ducreux, Oxaliplatin in colorectal cancer: an overview, Semin. Oncol. 27 (2000) 96–104.
[17] B. Stordal, N. Pavlakis, R. Davey, Oxaliplatin for the treatment of cisplatin-resistant cancer: a systematic review, Cancer Treat. Rev. 33 (2007) 347–357.
[18] Wu, H. Li, R. Liu, X.-Q. Gao, M.-H. Zhang, P.-X. Liu, Z. Fu, J.-N. Yang, D. Zhang-Negrerie, Q.-Z. Gao, Galactose conjugated platinum(II) complex targeting the Warburg effect for treatment of non-small cell lung cancer and colon cancer, Eur. J. Med. Chem. 110 (2016) 32–42.
[19] W.C. Johnson, CD of nucleic acids, in: K. Nakanishi, N. Berova, R.W. Woody (Eds.), Circular Dichroism: Principles and Applications, VCH, New York, 1994, p. 523.
[20] M.J. Waring, Complex formation between ethidium bromide and nucleic acids, J. Mol. Biol. 13 (1965) 269–282.
[21] S. De Jong, J.G. Zulstra, H. Timmer-Bosscha, N.H. Mulder, E.G. de Vries, Detection of DNA cross-links in tumor cells with the ethidium bromide fluorescence assay, Int. J. Cancer 37 (1986) 557–561.
[22] C. Ji, L.-Y. Zhang, S.-X. Dou, P.-Y. Wang, Local conformation transitions of linear DNA induced by cisplatin, Chin. Sci. Bull. 59 (2014) 3085–3089.
[23] G.B. Onoa, V. Moreno, Study of the modifications caused by cisplatin, transplatin, and Pd(II) and Pt(II) mepirizole derivatives on pBR322 DNA by atomic force microscopy, Int. J. Pharm. 245 (2002) 55–65.
[24] H.-Y. Zhang, C. Ji, Y.-R. Liu, W. Li, H. Li, S.-X. Dou, W.-C. Wang, L.-Y. Zhang, P. Xie, P.-Y. Wang, Effects of pH on oxaliplatin-induced condensation of single DNA molecules, Chin. Phys. Lett. 31 (2014) 028701.
[25] L.-P. Li, R.-S. Liu, F.-J. Xu, Y.-G. Zu, Z.-G. Liu, Study on the interactions between anti-cancer drug oxaliplatin and DNA by atomic force microscopy, Micron 76 (2015) 46–51.
[26] D. Jaganyi, A. Hofmann, R. van Eldik, Controlling the lability of square-planar Pt (II) complexes through electronic communication between pi-acceptor ligands, Angew. Chem., Int. Ed. Engl. 40 (2001) 1680–1683.
[27] T. Ishikawa, F. Ali-Osman, Glutathione-associated cis-diamminedichloroplatinum (II) metabolism and ATP-dependent efflux from leukemia cells. Molecular characterization of glutathione-platinum complex and its biological significance, J. Biol. Chem. 268 (1993) 20116–20125.
[28] G. Zaman, J. Lankelma, O. van Tellingen, J. Beijnen, H. Dekker, C. Paulusma, R. P. Oude Elferink, F. Baas, P. Borst, Role of glutathione in the export of compounds from cells by the multidrug-resistance-associated protein, Proc. Natl. Acad. Sci. U. S. A. 92 (1995) 7690–7694.
[29] K.S. Lovejoy, R.C. Todd, S. Zhang, M.S. McCormick, J.A. D'Aquino, J.T. Reardon, A. Sancar, K.M. Giacomini, S.J. Lippard, cis-Diammine(pyridine)chloroplatinum (II), a monofunctional platinum(II) antitumor agent: uptake, structure, function, and prospects, Proc. Natl. Acad. Sci. U. S. A. 105 (2008) 8902–8907.
[30] S. Dedola, D.L. Hughes, S.A. Nepogodiev, M. Rejzek, R.A. Field, Synthesis of alpha- and beta-D-glucopyranosyl triazoles by CuAAC 'click chemistry': reactant tolerance, reaction rate, product structure and glucosidase inhibitory properties, Carbohydr. Res. 345 (2010) 1123–1134.